

Improved hybrid functional for solids: The HSEsol functional

Laurids Schimka, Judith Harl, and Georg Kresse

Citation: *The Journal of Chemical Physics* **134**, 024116 (2011); doi: 10.1063/1.3524336

View online: <http://dx.doi.org/10.1063/1.3524336>

View Table of Contents: <http://scitation.aip.org/content/aip/journal/jcp/134/2?ver=pdfcov>

Published by the [AIP Publishing](#)

Articles you may be interested in

[A DFT study on structural, vibrational properties, and quasiparticle band structure of solid nitromethane](#)
J. Chem. Phys. **138**, 184705 (2013); 10.1063/1.4803479

[Range separated hybrid density functional with long-range Hartree-Fock exchange applied to solids](#)
J. Chem. Phys. **127**, 054101 (2007); 10.1063/1.2759209

[Why does the B3LYP hybrid functional fail for metals?](#)
J. Chem. Phys. **127**, 024103 (2007); 10.1063/1.2747249

[Screened hybrid density functionals applied to solids](#)
J. Chem. Phys. **124**, 154709 (2006); 10.1063/1.2187006

[Efficient hybrid density functional calculations in solids: Assessment of the Heyd–Scuseria–Ernzerhof screened Coulomb hybrid functional](#)
J. Chem. Phys. **121**, 1187 (2004); 10.1063/1.1760074



AIP | Journal of
Applied Physics

Journal of Applied Physics is pleased to
announce **André Anders** as its new Editor-in-Chief

Improved hybrid functional for solids: The HSEsol functional

Laurids Schimka,^{a)} Judith Harl, and Georg Kresse

University of Vienna, Faculty of Physics, and Center for Computational Materials Science, Sensengasse 8/12, A-1090 Vienna, Austria

(Received 31 August 2010; accepted 15 November 2010; published online 13 January 2011)

We introduce the hybrid functional HSEsol. It is based on PBEsol, a revised Perdew–Burke–Ernzerhof functional, designed to yield accurate equilibrium properties for solids and their surfaces. We present lattice constants, bulk moduli, atomization energies, heats of formation, and band gaps for extended systems, as well as atomization energies for the molecular G2-1 test set. Compared to HSE, significant improvements are found for lattice constants and atomization energies of solids, but atomization energies of molecules are slightly worse than for HSE. Additionally, we present zero-point anharmonic expansion corrections to the lattice constants and bulk moduli, evaluated from *ab initio* phonon calculations. © 2011 American Institute of Physics. [doi:10.1063/1.3524336]

I. INTRODUCTION

Density functional theory (DFT) in the formulation of Kohn and Sham (KS)¹ provides an efficient method to evaluate materials properties on a quantum-mechanical level. The present approximations to the exchange–correlation energy, however, lead to systematic errors in the description of geometrical properties, atomization energies, heats of formation, surface energies, and adsorption energies. For example the widely used local density approximation (LDA) and the gradient corrected Perdew–Burke–Ernzerhof (PBE)² functional yield average errors of approximately 1%–2% in the lattice constants; LDA underestimates, while PBE overestimates them. In addition, PBE lattice constant errors systematically increase with increasing mass (e.g., along the series C, Si, Ge, α -Sn). On the other hand, errors in the LDA atomization energies (compound energy vs. atomic energy) are often exceeding 100 kJ/mol, and although PBE improves the performance for the atomization energies significantly, for heats of formation the errors often remain as large as 50 kJ/mol per formula unit (f.u.).³

An alternative approach is based on a (partial) exact treatment of the exchange energy. In most cases, it is favorable to mix only a fraction of the non-local exact exchange to a (semi)-local exchange expression.⁴ These so called hybrid functionals (e.g., the PBE0^{5,6} functional by Perdew, Burke, and Ernzerhof) also offer a better description of band gaps as they can be considered as an approximation to the GW quasi-particle equation assuming a static, fixed dielectric function.

For solids, where the long-range part of the exact exchange is screened by correlation effects, faster numerical convergence of the hybrid functionals with k-points can be obtained by splitting the Coulomb interaction v into a short-range (SR) and long-range (LR) part, e.g., by defining

$$v(r) = \frac{1}{r} = \underbrace{\frac{\text{Erf}(\mu r)}{r}}_{v^{LR}} + \underbrace{\frac{\text{Erfc}(\mu r)}{r}}_{v^{SR}}, \quad (1)$$

^{a)} Author to whom correspondence should be addressed. Electronic mail: laurids.schimka@univie.ac.at. URL: <http://cms.mpi.univie.ac.at>.

and by evaluating the long range part using DFT. In the screened hybrid functional introduced by Heyd, Scuseria, and Ernzerhof (HSE),⁷ one quarter of the PBE short-range exchange is replaced by the exact exchange and the full PBE correlation energy is added. In the HSE06 functional (HSE06)⁸ the range-separation parameter μ is set to $\mu = 0.207 \text{ \AA}^{-1}$, yielding a well balanced description for many properties.

Calculations of the lattice constants show that the fractional inclusion of exact exchange provides an improved description compared to the underlying semi-local PBE functional.^{8,9} However, HSE06 inherits the PBE tendency to overestimate lattice constants, as well as the increase of the error for heavier elements. This overestimation can be pronounced for metals (e.g., Ag error 2%), ionic compounds (LiF, LiCl, NaF, NaCl approx. 1%), and heavier elements (α -Sn error > 1.2%).¹⁰ In addition, for transition metals, the atomization energies of solids exhibit significantly increased errors compared to PBE. In this paper, we introduce a hybrid functional, HSEsol, which has the same form and the same range-separation parameter as the HSE06 functional, but is based on the PBEsol¹¹ functional for the semi-local exchange and correlation part:

$$E_{xc}^{\text{HSEsol}} = E_c^{\text{PBEsol}} + E_x^{\text{PBEsol}} - \frac{1}{4} E_x^{\text{SR,PBEsol}} + \frac{1}{4} E_x^{\text{SR,EXX}}. \quad (2)$$

A more detailed description of HSEsol and results for solids will be presented in Sec. II A and Secs. III A–III C, respectively. We note that the PBEsol functional yields very similar results as the AM05 functional suggested by Armiento and Mattsson in 2005,^{12,13} and we could have equally well have based our new functional on AM05. However, the lack of an explicit formula for the AM05 exchange hole precluded such a development.

Moreover, we present *ab initio* calculations of the zero-point anharmonic expansion (ZPAE) effect on the lattice constants. The increase of the theoretical lattice constants caused by the ZPAE can be as large as 2% for very light solids such as LiH. The influence on Li is still 0.7% and

TABLE I. Parameters of the PAW data sets used in the present work, but not in Ref. 9. "Valence" indicates which orbitals are treated as valence orbitals; r_c^l are the cutoff radii for the partial waves. If small indices are used, they indicate which cutoff was used for s -, p -, and d -partial waves. E_{cut} are the energy cutoffs used in the present work.

	Valence	r_c^l (a.u.)	E_{cut} (eV)
H	1s	0.8	700
Be	1s2s	1.5 _s , 1.8 _{pd}	310
S	3s3p	1.5	400
Ge	3d4s4p	2.3 _{sp} , 2.2 _d	310
In	4d5s5p	2.5	240
Sn	4d5s5p	2.5	240
Sb	5s5p	2.3	170

0.5–0.9 % for LiF, LiCl, and NaCl. In view of new methods like PBEsol, AM05,^{12,14} revTPSS,¹⁵ the random-phase approximation (RPA),^{3,16} or the second-order screened exchange corrected RPA,¹⁷ that all yield average lattice constant errors as small as 0.5%, it is evident that the effect of the ZPAE must not be neglected. The ZPAE is often accounted for by semi-empirical formulas as derived in Ref. 18. The *ab initio* evaluation of zero-point energies via the phonon density of states is well established. In the context of *ab initio* calculations, such corrections have been first calculated for BN¹⁹ and MgO.²⁰ Nowadays, they can be routinely evaluated for the materials considered in performance tests of new functionals, however a concise set of zero point vibration corrections is yet not available for solids. The ZPAE evaluated from *ab-initio* via the calculation of phonon frequencies is discussed in Sec. II B. The results will be compared to the ZPAE corrections calculated using a the semi-empirical formula given in Ref. 18.

II. METHOD OF CALCULATION

All results presented in this paper have been obtained using the projector augmented-wave method^{21,22} as implemented in the Vienna *Ab Initio* Simulation Package (VASP).^{23,24}

The evaluation of the exact exchange energy in VASP as required for the HSE and the HSEsol functional has been discussed in Refs. 9 and 25. The PAW potentials used in the present work are equal to the ones in Ref. 9. Parameters of the PAW potentials of elements not included in Ref. 9 are summarized in Table I.

A. The HSEsol functional

For the HSEsol functional, one quarter of the short-range PBEsol exchange is replaced by the exact exchange. The short-range PBEsol exchange can be calculated by multiplying the LDA exchange energy density with the enhancement factor $F_x^{SR, \text{PBEsol}}(s, \mu/k_F)$, which depends on the dimensionless reduced gradient $s = |\nabla n|/(2k_F n)$ and the reduced range-separation parameter μ/k_F , $k_F = (3\pi^2 n)^{1/3}$

(see, e.g., Ref. 26):

$$E_x^{SR, \text{PBEsol}} \quad (3)$$

$$= \int d^3r n(\mathbf{r}) \epsilon_x^{\text{LDA}}[n(\mathbf{r})] F_x^{SR, \text{PBEsol}}(s(\mathbf{r}), \mu/k_F(\mathbf{r})). \quad (4)$$

The enhancement factor is determined by an integral of the range-separated Coulomb kernel $v^{SR} = \text{Erfc}(\mu u)/u$ times the spherically-averaged PBEsol exchange hole along $y = k_F u$:

$$F_x^{SR, \text{PBEsol}, \mu}(s, \mu/k_F) = -\frac{8}{9} \int_0^\infty dy y J^{\text{PBEsol}}(s, y) \text{Erfc}((\mu/k_F) y). \quad (5)$$

For the PBEsol exchange hole, we use the form recently proposed by Henderson–Janesko–Scuseria (HJS)^{27,28} as formulated for the PBEsol functional. In the HSE functional as defined in Refs. 7 and 29, the PBE exchange hole by Perdew *et al.*²⁶ has been applied. In contrast to that PBE²⁶ hole and the recently proposed PBEsol³⁰ exchange correlation hole by Perdew *et al.*, the HJS exchange hole allows a fully analytical evaluation of the range-separated enhancement factor. Additionally, it reproduces the PBE and PBEsol exchange energy, if the unscreened Coulomb kernel is used.

The short-range exact exchange energy is obtained by replacing the Coulomb kernel in the exact exchange energy expression. The SR exact exchange is accordingly given as a double-sum over all occupied (occ) one-electron states $\psi_i(\mathbf{r})$:

$$E_x^{SR, \text{EXX}} = -\frac{1}{2} \sum_{ij, \text{occ}} \int d^3r d^3r' v^{SR}(|\mathbf{r} - \mathbf{r}'|) \times \psi_i^*(\mathbf{r}) \psi_j(\mathbf{r}) \psi_j^*(\mathbf{r}') \psi_i(\mathbf{r}'). \quad (6)$$

The one-electron Schrödinger equation is solved with the corresponding non-local exchange potential

$$V_x(\mathbf{r}, \mathbf{r}') = - \sum_{j, \text{occ}} v^{SR}(|\mathbf{r} - \mathbf{r}'|) \times \psi_j(\mathbf{r}) \psi_j^*(\mathbf{r}').$$

The convergence with respect to the k -point grid used in the BZ sampling is the same as for the HSE06 functional and we therefore refer to the detailed tests shown in Ref. 9. HSEsol lattice constants are presented in Sec. III A and the atomization energies and heats of formation are presented in Sec. III B. Γ -centered Monkhorst-Pack like k -point grids were employed: $12 \times 12 \times 12$ k -points for insulators and $20 \times 20 \times 20$ k -points for metals. The reciprocal grid for the exact-exchange potential has been down sampled by a factor of two.³¹

B. Zero-point anharmonic expansion correction from *ab initio*

Experimental lattice constants are affected by contributions from phonon zero point vibration energies, which are in general not accounted for in zero temperature DFT calculations. Zero-point vibration energies influence not only the

TABLE II. PBE lattice constants without (first column) and with (second column) zero-point vibrational energies. The change due to the resulting correction with respect to experiment is shown in column five and seven. The experimental $T = 0$ K lattice constants and the experimental lattice constants corrected for by the semi-empirical ZPAE given in Eq. (9) have been taken from Ref. 32 (third and fourth column). The sixth column shows the experimental lattice constants corrected for by the PBE ZPAE calculated from *ab initio* phonon calculations. All lattice constants are given in Å. The Strukturbericht symbols (in parentheses) are used for the structure as follows: A1-fcc; A2-bcc; A4-diamond; B1-rocksalt; B3-zinc blende.

Solid	PBE	PBE+ZPAE corr	Exp.	Exp-ZPAE (empirical)	% to Exp	Exp-ZPAE (present)	% to Exp
Li(A2)	3.437	3.461	3.477	3.451	0.7	3.453	0.7
Na(A2)	4.197	4.208	4.225	4.209	0.4	4.214	0.3
Al(A1)	4.040	4.054	4.032	4.019	0.3	4.018	0.3
Rh(A1)	3.830	3.835	3.798	3.793	0.1	3.794	0.1
Pd(A1)	3.943	3.948	3.881	3.876	0.1	3.876	0.1
Cu(A1)	3.636	3.643	3.603	3.596	0.2	3.595	0.2
Ag(A1)	4.147	4.154	4.069	4.062	0.2	4.062	0.2
C(A4)	3.573	3.586	3.567	3.544	0.6	3.553	0.4
Si(A4)	5.469	5.478	5.430	5.415	0.3	5.421	0.2
Ge(A4)	5.761	5.769	5.652	5.639	0.2	5.644	0.1
Sn(A4)	6.656	6.664	6.482	6.474	0.1	6.474	0.1
LiH(B1)	4.006	4.090	4.064			3.979	2.1
LiF(B1)	4.064	4.102	4.010	3.960	1.2	3.972	0.9
LiCl(B1)	5.148	5.184	5.106	5.072	0.7	5.070	0.7
NaF(B1)	4.706	4.733	4.609	4.576	0.7	4.582	0.6
NaCl(B1)	5.699	5.724	5.595	5.565	0.5	5.569	0.5
MgO(B1)	4.260	4.278	4.207	4.186	0.5	4.189	0.4
SiC(B3)	4.379	4.391	4.358	4.340	0.4	4.346	0.3
BN(B3)	3.626	3.641	3.607	3.585	0.6	3.592	0.4
BP(B3)	4.547	4.560	4.538	4.520	0.4	4.525	0.3
BAs(B3)	4.808	4.830	4.777	4.760	0.4	4.755	0.5
GaN(B3)	4.546	4.557	4.520	4.509	0.2	4.509	0.2
GaP(B3)	5.506	5.515	5.448	5.435	0.2	5.439	0.2
GaAs(B3)	5.752	5.760	5.648	5.637	0.2	5.640	0.1
AlN(B3)	4.402	4.414	4.380			4.368	0.3
AlP(B3)	5.506	5.516	5.460	5.445	0.3	5.451	0.2
AlAs(B3)	5.735	5.743	5.658	5.646	0.2	5.649	0.2
InP(B3)	5.962	5.971	5.866	5.856	0.2	5.858	0.1
InAs(B3)	6.192	6.199	6.054	6.044	0.2	6.047	0.1
InSb(B3)	6.638	6.644	6.479	6.471	0.1	6.473	0.1

absolute energy but also the equation of state (energy versus volume curve), because the phonon frequencies decrease with increasing volume. This zero-point anharmonic expansion (ZPAE) has to be taken into account for an accurate comparison of theoretical and experimental lattice constants. To estimate the ZPAE, the PBE lattice constants of the materials presented in Table II are evaluated as the minimum of the internal energy $U(V)$ versus volume V curves

$$U(V) = E_0(V) + U_{\text{zero}}(V) \quad (7)$$

and as the minimum of the electronic contribution $E_0(V)$ only. The zero-point vibrational energy is calculated as a frequency integration over the vibrational density of states $g(V, \omega)$:

$$U_{\text{zero}}(V) = \frac{1}{2} \int \hbar \omega g(V, \omega) d\omega. \quad (8)$$

We use a direct approach employing the force constant method as outlined in Ref. 33 to calculate the phonon dispersion relation and vibrational density of states $g(V, \omega)$ from *ab initio*. In this work, *ab initio* calculations were

performed using $2 \times 2 \times 2$ conventional unit cells and a plane-wave energy cutoff approximately 30 % above the default value. Convergence is reached at $4 \times 4 \times 4$ k-points for insulators and semi-conductors and at $8 \times 8 \times 8$ k-points for metals, with the exception of Li, which requires a $12 \times 12 \times 12$ k-point grid. Figure 1 visualizes the effect of the zero-point vibrations for the case of C. The energy versus volume curve resulting from electronic contributions only as well as the zero-point corrected curve are shown. Beside shifting the energy-volume curve to smaller binding energies, the addition of the zero-point vibrational energies leads to an increase of the lattice constants resulting from the anharmonic potential. The effect of the specific functional (e.g. LDA versus PBE) on the zero-point vibrational effect is found to be negligible. To show this, we evaluated the zero-point energies applying the LDA functional for some selected materials. For the vibrational frequencies, the deviations from PBE are typically only about 5%, and the resultant change of the ZPAE corrected lattice constants is typically only 0.05 % (5% of 1%). This suggests that it is irrelevant whether the ZPAE are calculated using the PBE functional or using a more accurate

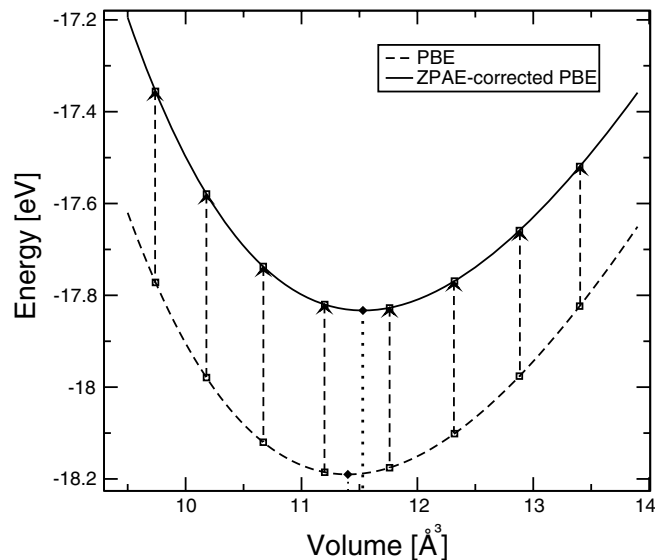


FIG. 1. Energy vs volume for C-diamond including the zero-point vibrational energy (bold line) and neglecting zero-point vibrational effects (dashed line).

functional. Before commenting on the results in more detail, we would like to compare our results with existing literature data. Grabowski *et al.* have also calculated zero point vibrational energies for few non magnetic fcc metals³⁴ using DFT within the quasi harmonic approximation. Their corrections for Al, Cu, Rh, Pd, Ag and Pt are essentially identical to our corrections. This is not astonishing, since similar codes and procedures were used, but it indicates that the authors of Ref. 34 and we have both reached technical convergence. The more interesting comparison is with the widely used semi empirical ZPAE corrections derived in Ref. 18:

$$\frac{\Delta a_0}{a_0} = \frac{\Delta V_0}{3 V_0} = \frac{3}{16}(B_1 - 1) \frac{k_B \Theta_D}{B_0 V_0}. \quad (9)$$

In this equation, the lattice constants a_0 , the bulk moduli B_0 , and the Debye temperatures Θ_D are usually obtained from experiment, whereas the pressure derivative of the bulk modulus B_1 is usually calculated and thus depends on the applied functional. It is immediately obvious, that the semi empirical formula is remarkably accurate (see Table II), *a posteriori* validating its use. In particular for metals, our present values are practically identical to the simpler empirical correction. For semiconductors and insulators, however, the empirical ZPAE corrections are slightly too large, specifically for C, BN, LiF or MgO the empirical formula overestimates the ZPAE by about 30%. This is most likely related to optical modes, which can not be properly described in the simple Debye model underlying Eq. (9).

In Table II corrected and uncorrected PBE lattice constants are summarized for our test set of materials. As already mentioned above LDA ZPAE corrections would be almost identical to PBE ZPAE corrections. It seems therefore reasonable to correct the experimental lattice constants directly, and to compare with those corrected experimental lattice constants from now on, instead of applying the corrections to the theoretical energy-volume curves. This is the route we will

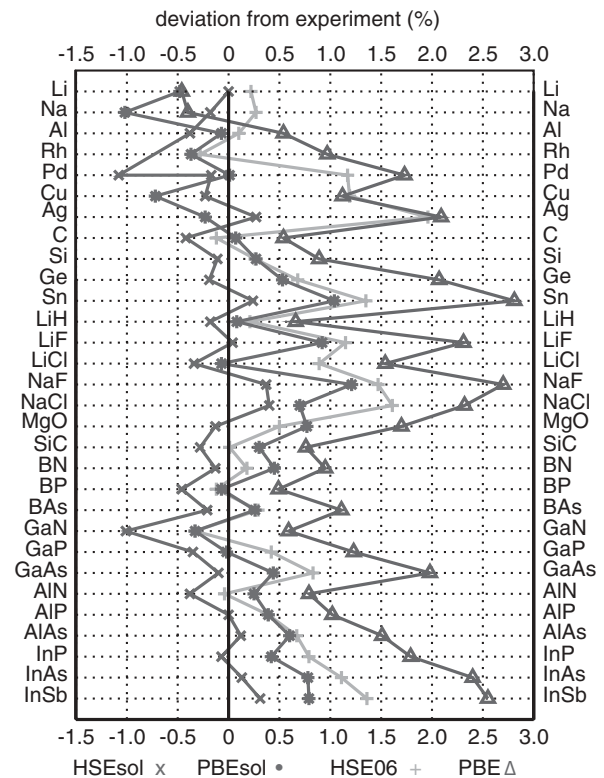


FIG. 2. Lattice constant errors (%) compared to the ZPAE corrected experimental lattice constant (see Sec. II B).

take from now on (see Table III for the corrected experimental lattice constants).

III. RESULTS

A. HSEsol lattice constants and bulk moduli

Lattice constants obtained from the HSEsol functional are summarized in Table III and are compared to PBE, PBEsol, and HSE06 values, whereas detailed results for the bulk moduli can be found in the supplementary material.³⁵ The lattice constant errors (%) with respect to the ZPAE corrected experimental values are visualized in Fig. 2 (see also the supplementary material for alternative representations of the same data).³⁵ While the PBE functional predicts overall too large lattice constants (with the exception of Na and Li), both HSE06 and PBEsol reduce the lattice constants and improve agreement with experiment. Compared to ZPAE corrected experimental lattice constants, the PBEsol and the HSE06 lattice constants are however still too large. The HSEsol functional provides smaller mean relative errors than the three other functionals, and only for Rh and GaN the error in the HSEsol lattice constants is larger than 1%. The bulk moduli are predicted to be slightly too large for HSEsol, but again, the HSEsol functional yields the smallest deviation from experiment (MARE: PBE 12.6%, PBEsol 6.6%, HSE 6.7%, HSEsol 4.0%). We note that the comparison was done with zero-point corrected bulk moduli by subtracting the zero-point corrections calculated for the PBE functional from the experimental values. This is certainly an approximation, but

TABLE III. Theoretical lattice constants (\AA) using the PBE, PBEsol, HSE, and the HSEsol functional. The PBE and HSE06 lattice constants equal the ones given in Ref. 9. The experimental lattice constants are taken from Ref. 32 and *ab initio* ZPAE corrections have been subtracted (see Table II).

Solid	Lattice constant (\AA)								
	PBE	%	PBEsol	%	HSE06	%	HSEsol	%	Exp
Li (A2)	3.437	-0.46	3.436	-0.48	3.460	0.22	3.453	0.00	3.453
Na (A2)	4.197	-0.40	4.171	-1.02	4.225	0.27	4.206	-0.18	4.214
Al (A1)	4.040	0.54	4.015	-0.07	4.022	0.10	4.003	-0.38	4.018
Rh (A1)	3.830	0.97	3.780	-0.37	3.783	-0.28	3.753	-1.08	3.794
Pd (A1)	3.943	1.73	3.876	0.01	3.921	1.17	3.869	-0.17	3.876
Cu (A1)	3.636	1.12	3.570	-0.72	3.638	1.19	3.587	-0.23	3.595
Ag (A1)	4.147	2.09	4.053	-0.23	4.142	1.96	4.073	0.27	4.062
C (A4)	3.573	0.54	3.556	0.07	3.549	-0.12	3.538	-0.42	3.553
Si (A4)	5.469	0.89	5.436	0.27	5.435	0.26	5.415	-0.11	5.421
Ge (A4)	5.761	2.07	5.674	0.53	5.682	0.68	5.633	-0.19	5.644
Sn (A4)	6.656	2.81	6.541	1.04	6.561	1.35	6.489	0.24	6.473
LiH(B1)	4.006	0.66	3.983	0.08	3.988	0.21	3.972	-0.18	3.979
LiF (B1)	4.064	2.31	4.009	0.92	4.018	1.15	3.974	0.04	3.972
LiCl (B1)	5.148	1.54	5.066	-0.07	5.115	0.89	5.052	-0.34	5.070
NaF (B1)	4.706	2.70	4.638	1.21	4.650	1.47	4.599	0.37	4.582
NaCl (B1)	5.699	2.32	5.608	0.70	5.659	1.61	5.592	0.40	5.569
MgO(B1)	4.260	1.70	4.222	0.77	4.210	0.50	4.184	-0.13	4.189
SiC(B3)	4.379	0.76	4.359	0.30	4.347	0.01	4.334	-0.28	4.346
BN(B3)	3.626	0.95	3.608	0.45	3.598	0.18	3.587	-0.13	3.592
BP(B3)	4.547	0.49	4.521	-0.07	4.519	-0.12	4.504	-0.46	4.525
BA3(B3)	4.808	1.11	4.767	0.26	4.769	0.29	4.745	-0.21	4.755
GaN (B3)	4.546	0.83	4.494	-0.32	4.494	-0.33	4.464	-1.01	4.509
GaP (B3)	5.506	1.23	5.438	-0.02	5.462	0.42	5.420	-0.35	5.439
GaAs (B3)	5.752	1.98	5.665	0.44	5.687	0.83	5.635	-0.10	5.640
AlN(B3)	4.402	0.79	4.378	0.25	4.366	-0.04	4.351	-0.38	4.368
AlP(B3)	5.506	1.02	5.472	0.39	5.472	0.39	5.450	0.00	5.451
AlAs(B3)	5.735	1.51	5.683	0.60	5.687	0.67	5.656	0.12	5.649
InP (B3)	5.962	1.79	5.882	0.42	5.904	0.79	5.854	-0.07	5.858
InAs (B3)	6.192	2.40	6.094	0.78	6.114	1.11	6.055	0.13	6.047
InSb (B3)	6.638	2.55	6.524	0.79	6.561	1.36	6.493	0.31	6.473
ME	0.068		0.013		0.031		-0.006		
MRE		1.35%		0.23%		0.61%		-0.15%	
MAE	0.071		0.022		0.033		0.013		
MARE		1.41%		0.46%		0.67%		0.28%	

such corrected bulk moduli are convenient to evaluate the performance of other functionals.

A characteristic feature of the PBE functional is the increase of the error in the lattice constants for heavier solids. This can be seen, e.g., along the series: C-Si-Ge- α -Sn, GaN-GaP-GaAs or InP-InAs-InSb. The PBEsol and HSE06 functionals follow this trend as well, but with a reduced slope in the lattice constant error. HSEsol reduces the slope for the C-Si-Ge- α -Sn even further. For GaN-GaP-GaAs, it performs slightly worse than PBEsol (but better than HSE06), whereas for InP-InAs-InSb, the slope is similar to PBEsol (and smaller than for HSE06).

B. HSEsol atomization energies and heats of formation

Ideally, a functional should provide reasonable atomization energies for molecules *and* extended systems. This goal is very difficult to achieve using density or hybrid functionals. Generally, the PBE functional overestimates the stability

of molecules, and it underestimates the stability of solids. By changing the density functional, one can either increase or decrease the atomization energies, but it is not possible to get solids and molecules right simultaneously using simple gradient corrected functionals. As we will see, replacing part of the density functional theory exchange by exact exchange also reduces the atomization energies (to a large extent this is related to an increased spin-polarization energy of the atoms), but again it is not possible to improve the description of solids and molecules simultaneously.

In this section, we present atomization energies for molecules (G2-1 set at PBE0 geometries for 55 molecules) in Table VI and for extended systems in Table V using the PBE, PBEsol, HSE and HSEsol functionals. Heats of formations with respect to the components under ambient conditions are summarized in Table IV.

The two semi-local functionals, PBE and PBEsol, significantly overbind molecules in the G2-1 test set (Table VI). The average PBE atomization energies are closer to experiment (ME 27 kJ/mol) than the PBEsol atomization energies

TABLE IV. Heats of formation at $T = 0$ K in kJ/mol (per formula unit; 1 kJ/mol = 10.364 meV) with respect to the elemental phases in their normal state under ambient conditions. Experimental values are collected in Ref. 36 and have been corrected for zero-point vibrations (ZPV, experimental values without corrections are in parentheses). The ZPV have been evaluated using harmonic *ab initio* phonon calculations.

Solid	PBE	PBEsol	HSE06	HSEsol	RPA	Exp.
LiF	569	573	591	599	609	619 (614)
NaF	522	522	540	546	567	577 (573)
NaCl	355	355	371	374	405	413 (411)
SiC	52	53	60	60	64	69 (72)
AlN	260	280	286	303	291	321 (313)
MgH ₂	52	60	64	72	72	78 (68)
MgO	517	533	541	558	577	604 (597)
ME	-51	-44	-33	-24	-14	

(ME 70 kJ/mol). Adding exact exchange reduces the mean error for both functionals to -5 kJ/mol (HSE) and 29 kJ/mol (HSEsol). We note that the reduction of the binding energy is pretty similar for both functionals amounting to about 30 kJ/mol, and it is clear that the HSE06 functional performs significantly better than the HSEsol functional.

For the extended systems (Table V), on the other hand, the PBE functional performs already quite well (ME -12 kJ/mol). Contrary to small molecules, solids are underbound on average. In this case, adding non-local exchange can make the situation only worse, resulting in significant underbinding (ME -22 kJ/mol). For metals, the performance of the HSE06 functional is, in fact, particularly bad with the worst cases being transition metals. While PBE provides a very reasonable atomization energy for them (6 and 22 kJ/mol for Rh and Pd), the error for the HSE06 hybrid functional is about 100 kJ/mol. As for molecules, PBEsol increases the atomization energies significantly with respect to the PBE values (ME 26 kJ/mol). In this case, adding non-local exchange helps to reduce the atomization energies back to very reasonable values (ME 4 kJ/mol) but unfortunately the mean absolute error remains large and very similar to the PBE case (HSEsol MAE 18 kJ/mol, PBE MAE 15 kJ/mol). A major reason for this is that HSEsol tends to underbind metals (ME -20 kJ/mol), but overbinds insulators and semiconductors (ME 11 kJ/mol). This reduces the mean error but also increases the mean absolute error.

Assessments based on atomization energies only are sometimes criticized for depending too much on the quality of the description of the atoms. We have thus selected a few gas phase/metal and solid/solid state reactions. To this end, the heats of formation of eight solid compounds are summarized in Table IV. Although PBE performs reasonably well for the atomization energies of solids, heats of formation are shockingly inaccurate (ME -51 kJ/mol). The likely and common explanation for this error is that the binding energy of dimers, O₂, N₂, F₂ etc. are overestimated (compare Table VI) but this does not explain the error for MgH₂ or SiC. For this particular test set, PBEsol performs slightly better than PBE, but it reduces the overbinding only by a few kJ (ME -44 kJ/mol). The two hybrid functionals perform better than the parent semi-local functionals (HSE06 ME -33 kJ/mol,

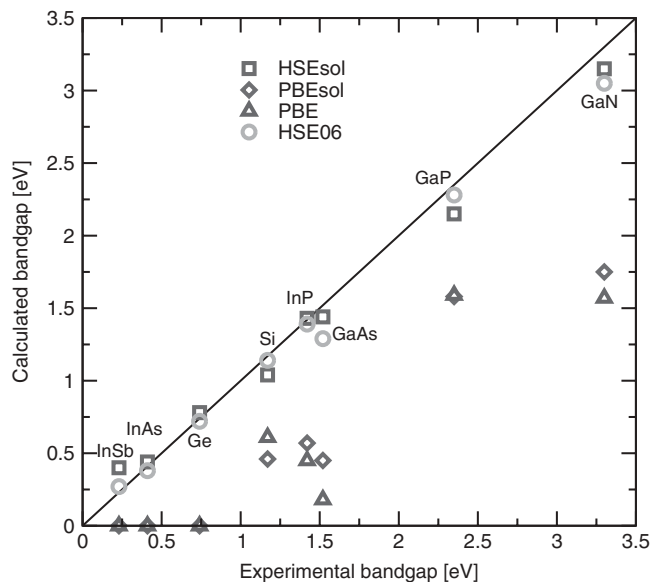


FIG. 3. Theoretical versus experimental band gaps for selected semiconductors. PBE and PBEsol band gaps are “negative” (inverted band characters at Γ) for InSb, InAs, Sn and Ge.

HSEsol ME -24 kJ/mol). The likely explanation for this observation is that hybrid functionals make the binding in metals weaker compared to the binding of the final (ionic) compounds. Simultaneously the bond-strength of the dimers is reduced by admixing non-local exchange, bringing the heats of formation in better agreement with experiment. However, none of the semi local or hybrid functionals perform as well as the RPA^{3,16} (RPA ME -14 kJ/mol), suggesting that the RPA is presently the best choice for predicting the thermo chemistry of solids, but matter of fact, the RPA is orders of magnitude more expensive than local or even hybrid functionals.

Overall, the atomization energies and heats of formation presented in this subsection suggest that HSEsol provides quite reasonable atomization energies (although far from chemical accuracy) for both molecules and extended systems, as well as, the best heats of formation (disregarding RPA) among the functionals presented in this work.

C. Band gaps

It is often argued that KS one electron band gaps do not need to match the experimental QP band gaps. This is certainly true from a fundamental point of view. For instance, it has been shown that even very accurate Kohn-Sham potentials yield one-electron (Kohn-Sham) band gaps that do not match the QP energies.³⁹ However, the exact KS energy functional and the exact KS exchange-correlation potential possess an integer discontinuity upon adding or removing electrons, which would allow to calculate the exact QP gap by adding and removing electrons from large supercells and taking appropriate energy differences.^{40,41} For local and semi-local density functionals, as well as, hybrid functionals, on the other hand, energy differences encountered upon adding electrons to or removing electrons from *Bloch states* are exactly equivalent to the one-electron energies of the Bloch states to

TABLE V. Atomization energies in kJ/mol/atom for solids applying the PBE, PBEsol, HSE06, and HSEsol functional. The last two columns summarize the experimental atomization energies (including the ZPE) and the ZPE corrected atomization energies, respectively. Experimental atomization energies for InP, InAs, InSb have been taken from Ref. 37, for Ge and Sn from Ref. 38, all other experimental atomization energies are from Ref. 36. Relative errors are calculated with respect to the ZPE corrected experimental atomization energies.

	PBE	%	PBEsol	%	HSE	%	HSEsol	%	exp	exp ZPE corr.
Li (A2)	155	-3	162	1	151	-6	156	-2	157	160
Na (A2)	104	-4	111	3	99	-8	105	-3	107	108
Al (A1)	331	0	368	11	331	0	354	7	327	331
Rh (A1)	552	-1	645	16	443	-21	475	-15	555	558
Pd (A1)	358	-6	427	12	285	-25	334	-12	377	380
Cu (A1)	336	-1	389	14	297	-13	334	-2	337	340
Ag (A1)	243	-15	297	3	229	-20	268	-7	286	288
ME Metals	-12		33		-47		-20			
MAE Metals	12		33		47		26			
MARE Metals		4.3%		8.7%		13.2%		6.8%		
C (A4)	744	2	797	9	734	1	775	6	711	728
Si (A4)	440	-3	479	6	442	-2	467	3	446	452
Ge (A4)	360	-5	400	6	360	-5	390	3	374	378
Sn (A4)	306	1	343	13	306	1	334	10	301	303
LiH (B1)	227	-5	236	-2	228	-5	236	-2	230	240
LiF (B1)	418	-3	432	0	408	-5	421	-2	425	430
LiCl (B1)	324	-6	340	-2	324	-6	338	-3	343	346
NaF (B1)	369	-4	382	0	358	-7	370	-4	379	383
NaCl (B1)	298	-7	311	-4	298	-7	309	-4	319	322
MgO (B1)	481	-4	513	2	473	-6	498	-1	497	502
SiC (B3)	618	-1	663	6	619	-1	650	4	612	625
BN (B3)	669	3	714	9	660	1	692	6	637	652
BP (B3)	511	3	552	11	509	3	538	8	486	496
BAAs (B3)	447		490		443		474			
GaN (B3)	424	-4	467	6	418	-5	450	2	432	439
GaP (B3)	337	-3	376	8	340	-2	368	6	343	348
GaAs (B3)	304	-6	343	7	304	-6	334	4	319	322
AlN (B3)	551	-2	586	4	544	-4	570	1	556	564
AlP (B3)	395	-5	427	3	398	-5	421	1	411	417
AlAs (B3)	356	-3	390	6	357	-3	382	4	365	369
InP (B3)	304	-9	371	11	306	-9	332	-1	331	335
InAs (B3)	279	-6	316	6	278	-6	307	3	294	297
InSb (B3)	255	-6	289	7	253	-7	280	3	269	271
ME Ins/sem.	-12		23		-14		11			
MAE Ins/sem	16		25		17		16			
MARE Ins/sem		4.2%		5.8%		4.4%		3.7%		
ME all	-12		26		-22		4			
MAE all	15		27		24		18			
MARE all		4.2%		6.5%		6.5%		4.4%		

which the electron is added or removed. For a more detailed discussion we refer to Cohen, Mori-Sanchez and Yang.⁴¹ From a fundamental point of view, one might argue that the flaw of the present KS-functionals is the lack of this integer discontinuity, but from a practical point of view, the origin of the flaw matters rather little. As long as the exchange correlation functional does not possess an integer discontinuity, it is a sensible test to compare KS one-electron energies with the fundamental band gap.^{42,43} If the KS one-electron energy differences do not match the experimental band gaps, the applied functional needs to be used with some care, in particular if defect states are modeled.⁴⁴⁻⁴⁷

While, fundamental band gaps obtained from the one-electron energies of local and semi-local functionals are con-

sistently too small, the admixture of exact exchange leads to an opening of the gap yielding good agreement with experiment. In Table VII, fundamental band gaps evaluated using the PBE, PBEsol, HSE06, and HSEsol functional are presented. For each functional, the lattice constant was set to the respective theoretical equilibrium lattice constant. As the PBE and PBEsol functionals predict similar band gaps, it can be expected that the HSE06 and the HSEsol band gaps are close to each other as well. This is in fact the case, as can be seen from the very similar average errors provided by the two hybrid functionals, HSE06 and HSEsol. Both hybrid functionals perform significantly better than the semi-local PBE and PBEsol functionals. Only for large gap insulators, hybrid functionals do not yield satisfactory results, essentially

TABLE VI. Atomization energies in kJ/mol/ formula unit for a small subset of molecules from the G2-1 test (+H₂) set. The mean errors have been calculated for the full G2-1 test set, which can be found in the supplementary material (Ref. 35).

	PBE	Deviation	PBEsol	Deviation	HSE06	Deviation	HSEsol	Deviation	exp
H ₂	438	-18	446	-10	437	-19	446	-10	456
C ₂ H ₂	1735	45	1798	107	1694	4	1744	53	1690
C ₂ H ₄	2390	39	2477	125	2361	10	2431	79	2351
C ₂ H ₆	2997	22	3109	134	2981	6	3071	96	2975
CO	1124	32	1167	75	1070	-22	1103	11	1092
CO ₂	1737	97	1825	184	1639	-2	1703	63	1640
Cl ₂	275	36	309	70	252	14	276	38	238
ClF	301	42	340	81	257	-2	286	27	259
F ₂	218	59	260	101	147	-12	179	20	159
Li ₂	83	-25	86	-23	81	-28	84	-24	109
LiF	579	-2	598	17	549	-33	566	-16	582
LiH	224	-19	230	-13	221	-22	228	-15	243
N ₂	1019	69	1046	97	945	-5	967	17	950
Na ₂	74	-6	74	-6	66	-14	67	-12	79
NaCl	392	-22	410	-4	387	-27	401	-14	414
O ₂	598	104	650	156	521	27	559	65	494
P ₂	508	22	539	54	467	-18	491	6	485
SO	591	80	633	123	535	25	566	55	510
SO ₂	1173	115	1260	202	1066	8	1130	71	1059
Si ₂	340	30	361	51	322	12	338	28	310
SiO	822	23	861	62	765	-34	795	-4	799
ME		27		70		-5		29	
MAE		36		71		15		32	

TABLE VII. Theoretical and experimental fundamental band gaps in eV. Theoretical band gaps are evaluated at the equilibrium lattice constant determined with the corresponding functional. Except for LiF, LiCl, NaF, and NaCl, experimental band gaps have been taken from Ref. 48.

	PBE	Error	PBEsol	Error	HSE	Error	HSEsol	Error	exp
C (A4)	4.12	-1.36	4.03	-1.45	5.31	-0.17	5.27	-0.21	5.48
Si (A4)	0.61	-0.56	0.46	-0.71	1.14	-0.03	1.04	-0.13	1.17
Ge (A4)	-	-	-	-	0.72	-0.02	0.78	0.04	0.74
Sn (A4)	-	-	-	-	0.2	-	0.22	-	-
LiH (B1)	2.98	-1.96	2.73	-2.21	3.97	-0.97	3.8	-1.14	4.94
LiF (B1)	8.85	-5.65	9.05	-5.45	11.47	-3.03	11.64	-2.86	14.5
LiCl (B1)	6.27	-3.13	6.34	-3.06	7.78	-1.62	7.70	-1.70	9.4
NaF (B1)	6.06	-5.44	6.16	-5.34	8.37	-3.13	8.46	-3.04	11.5
NaCl (B1)	4.98	-4.53	4.99	-4.51	6.41	-3.09	6.40	-3.10	9.5
MgO (B1)	4.42	-2.80	4.58	-2.64	6.51	-0.71	6.64	-0.58	7.22
SiC (B3)	1.37	-1.05	1.23	-1.19	2.23	-0.19	2.16	-0.26	2.42
BN (B3)	4.45	-1.77	4.28	-1.94	5.79	-0.43	5.7	-0.52	6.22
BP (B3)	1.24	-1.16	1.11	-1.29	1.94	-0.46	1.86	-0.54	2.4
BAAs (B3)	1.22	-0.24	1.09	-0.37	1.85	0.39	1.77	0.31	1.46
GaN (B3)	1.57	-1.73	1.75	-1.55	3.05	-0.25	3.15	-0.15	3.30
GaP (B3)	1.59	-0.76	1.58	-0.77	2.28	-0.07	2.15	-0.20	2.35
GaAs (B3)	0.18	-1.34	0.45	-1.07	1.29	-0.23	1.44	-0.08	1.52
AlN (B3)	3.3	-2.83	3.18	-2.95	4.55	-1.58	4.48	-1.65	6.13
AlP (B3)	1.63	-0.88	1.45	-1.06	2.29	-0.22	2.16	-0.35	2.51
AlAs (B3)	1.5	-0.73	1.34	-0.89	2.08	-0.15	1.97	-0.26	2.23
InP (B3)	0.45	-0.97	0.57	-0.85	1.39	-0.03	1.43	0.01	1.42
InAs (B3)	-	-	-	-	0.38	-0.03	0.44	0.03	0.41
InSb (B3)	-	-	-	-	0.27	0.04	0.40	0.17	0.23
ME		-1.83		-1.85		-0.69		-0.70	
MAE		1.83		1.85		0.74		0.76	

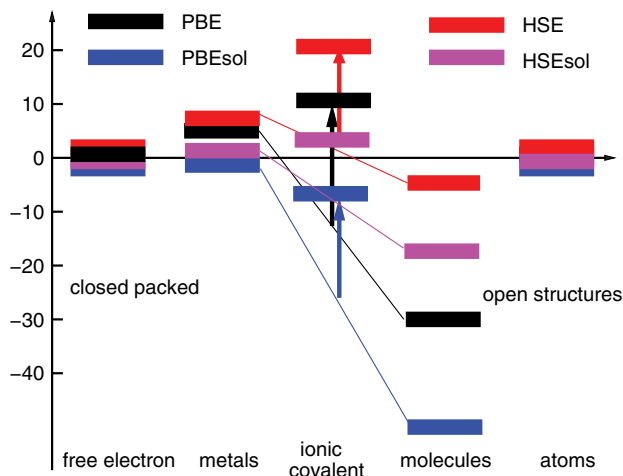


FIG. 4. Schematic presentation of the energy errors for PBE, HSE, PBEsol and HSEsol for selected systems. x-axis represents specific bonding situations. One bar is shown for each functional for each bonding situation. Each bar represents the total energy error for a specific functional and a specific situation. The lower a vertical bar is positioned the more strongly the specific functional overbinds. Bars above the x-axis correspond to underbinding for that specific situation.

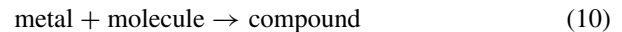
because one quarter of the exact exchange is insufficient to recover the correct band gap. In this case, half-half functionals yield somewhat better agreement with experiment, e.g. LiF (12.95 eV), NaF (9.47 eV) and NaCl (6.71 eV). However, the screening parameter μ is too large to allow for a better agreement with experiment.

IV. DISCUSSION

Figure 4 summarizes the energetics we have determined in the present work for PBE, HSE, PBEsol and HSEsol for *sp* elements in the first, second and third row. The plot is based on the atomization energy errors for molecules and solids shown in Tables VI and VII but restricts the statistics to simple metals (Na, Li, Al), ionic and covalent compounds (NaF, NaCl, AlN, . . .) and diatomic molecules (O_2 , F_2 , N_2 , P_2 , . . .). All energies are specified in kJ/mol per atom so that the graph essentially conveys the same content as the heats of formation shown in Table IV.

Since all functionals describe the energy of the free electron gas exactly, all four functionals fall onto a single line for this case (zero error in the total energy). The energies of atoms are more problematic, and, ideally, we would have liked to indicate the mean energy error for atoms for each functional in our plot. However, determining this error turned out to be rather cumbersome, since accurate atomic reference data are not available, in particular, if we want to assess the *valence electron* error only. We therefore aligned the atomic energies at zero, as well. Therefore, the y-position of each bar reflects the atomization energy error for metals, ionic and covalent solids and molecules, respectively. For each bonding situation we show 4 bars, corresponding to the error of the PBE, PBEsol, HSE and HSEsol functional. The presentation has been chosen such that negative values correspond to overbinding (different sign than in the tables).

Let us first concentrate on the PBE results (black bars). Clearly, PBE overestimates the atomization energies of small molecules significantly but slightly underestimates the atomization energies for metals, semiconductors and insulators. We note that real metals show a behavior in-between covalent solids and the free electron gas, which is sensible, since bonding in real metals is a mixture of covalent and free electron like bonding. One issue that is visible in the plot is that PBE significantly underestimates the heats of formation upon forming a compound from a metal and a gas phase molecule. As we have already discussed, the origin of the problem is the PBE overbinding for molecules. As a result, the heats of formation for the reaction



is underestimated, as indicated by the black arrow in Fig. 4.

With respect to atoms, PBEsol (blue bars) somewhat overbinds solids and strongly overbinds molecules. This is a result of aligning the energies for atoms at zero. In fact, the PBEsol functional yields smaller gradient corrections and thus less negative exchange correlation energies, but since the effect is strongest for atoms, molecules and solids are energetically overbound compared to atoms. Concerning the heats of formation of compounds w.r.t. metals and gas phase molecules, a slightly smaller error is observed for PBEsol than for PBE (blue arrow).

Hybrid functionals generally increase the stability of the spin polarized atom that we use as reference, and hence reduce the binding energy resulting in less negative atomization energies (red and pink bars). Remarkably, the changes in the atomization energies are largest for molecules, small for insulators and semiconductors, and fairly small for metals. This reflects a systematic difference between the local (DFT) and non-local (HF) exchange energy in extended and localized systems: whereas the difference is expected to be zero for the uniform electron gas, since all DFT functionals exactly reproduce the exchange energy of jellium, the difference is rather large for systems with localized electrons. We note that changes from PBEsol to HSEsol are larger than from PBE to HSE, suggesting that PBE models the exact exchange energy more precisely than PBEsol. In fact, functionals with even stronger gradient corrections, such as revPBE⁴⁹ and RPBE,⁵⁰ would be even better suited for molecules, but obviously such functionals would introduce too strong gradient corrections for extended systems, increasing their atomization energy error and lattice constant error even further beyond that of PBE.

An important question at this point is to what extent the diagram is biased by the restriction to a small set of the elements. This certainly is a difficult question that can be only addressed by increasing the test set further, but we believe that the general behaviour will not be affected by this choice: the stability of molecules is overestimated compared to bulk systems, regardless of the chosen (semi-local) density functional and test set. For instance, for Si (not included in the construction of the diagram) our PBE data show that the stability of the Si_2 dimer is overestimated by 30 kJ/mol, whereas the solid is underbound by 12 kJ/mol in rough agreement with our schematic energy plot. We thus conclude that the schematic diagram captures a true shortcoming of the presently

available semi-local and hybrid functionals, that is encountered when one moves from a uniform system to open structures with spatially confined electrons.

Which one is the best functional: The diagram suggests that there is no “best” functional. PBEsol is ideally suited for simple metals. For insulators and semiconductors, errors in the atomization energies are roughly similar but of opposite sign for PBE and PBEsol, and one would need a functional with intermediate gradient corrections. For molecules, even the PBE gradient corrections do not suffice to recover a reasonable energetics, and in fact, revPBE and RPBE with even stronger gradient corrections are known to achieve the best molecular energetics.⁴⁹ As Perdew has already pointed out, the strength of the gradient correction needs to be chosen system dependent, something that can be only achieved by including additional information as done in the TPSS or revTPSS functional.¹⁵

For hybrid functionals, the HSE functional does the best overall job for atomization energies of molecules, but HSEsol is best suited for solids. Again, none of the functionals is ideal. Tentatively, we believe that the proper physics can be only recovered by functionals that use the correct amount of the non-local exchange interaction, but the required fraction is system dependent: a sizeable amount of exact non-local exchange in molecules and atoms, and very little non-local exchange in solids would produce about the right energetics.

V. CONCLUSIONS

In this work, we have presented an improved hybrid functional for solids. In this functional, one quarter of the short-range semi-local exchange is replaced by exact exchange, analogous to HSE. In contrast to HSE, it relies on the PBEsol instead of the PBE functional for presenting the semi-local exchange part and the correlation energy. We note that similar functionals have been proposed for the modeling of ferroelectric materials, however, a careful evaluation of the performance of such functionals has not been presented yet.⁵¹

Our motivation to introduce a hybrid functional based on PBEsol is to improve the performance of hybrid functionals for solids. Although HSE06 yields very good atomization energies for molecular systems, errors in the lattice constants of solids can be sizable (e.g. 2% and 1.6% for Ag and NaCl, respectively, mean absolute relative error 0.7%). Accurate lattice constants are important for *ab initio* modeling since most physical quantities need to be evaluated at the theoretical geometry, if consistency is aimed at. Furthermore, in contrast to molecular systems, HSE06 atomization energies of solids are not improved compared to PBE.

The ideal hybrid functional for solids should yield better lattice constants (and bulk moduli) than HSE06, and it should improve the atomization energies for solids. At the same time, molecular atomization energies should not be significantly worsened, and the description of band gaps should remain similar to HSE06. The HSEsol functional provides all this: the mean absolute error in the lattice constants is reduced from 0.67% (HSE06) to 0.28%. For the systems studied in the present work, the largest lattice constant error is 1.1% (Rh) compared to the largest HSE06 error of 2.0 %

(Ag). For molecular atomization energies, the improvement provided by the HSEsol functional compared to the underlying PBEsol functional is of the same order as from PBE to the HSE06 functional. But because PBEsol performs significantly worse than PBE for molecules, the HSEsol results are not on par with the HSE06 results. This disadvantage of the HSEsol functional is, however, compensated by the improved HSEsol atomization energies of solids. For metallic systems, the HSE06 error is almost halved (from MARE 13.2% to 6.8%) and for insulators and semiconductors HSEsol performs also slightly better (HSE06: MARE 4.4%, HSEsol: MARE 3.7%). Additionally, HSEsol heats of formation (with respect to the constituents in their groundstate at ambient conditions) are closer to experiment than the HSE06 values. For the energetics of solids, HSEsol is thus seemingly a better choice than HSE06. Finally, band gaps are of comparable quality as for the HSE06 functional.

In summary, we believe that HSEsol provides an improved description of solids compared to HSE06. Specifically, the prediction of lattice constants and heats of formations is much improved.

A second issue discussed in this work is the *ab initio* calculation of the zero-point vibrational effects on the atomization energies and of the zero-point anharmonic expansion contributions to the lattice constants and bulk moduli. In first principles calculations, these effects are a priori not taken into account for the calculation lattice constants and atomization energies, hence, it would be most convenient to correct the experimental values for zero-point effects in order to precisely determine the accuracy of a functional. The zero-point effect on the lattice constants is on average about 0.3 % (LiH excluded) and is therefore in the range of error of accurate methods such as the HSEsol functional. In this work, we presented zero-point anharmonic expansion effects calculated from *ab initio* phonon calculations based on the quasi harmonic approximation. Although the evaluation of zero-point energies is straightforward, to the best of our knowledge zero-point anharmonic expansion effects have not yet been presented for a larger set of solids. The values presented in this work can be used as a generic correction for the experimental lattice constants and bulk moduli.

ACKNOWLEDGMENTS

This work has been supported by the Austrian Fonds zur Förderung der wissenschaftlichen Forschung within the Wissenschaftskolleg W4 and the START project Y218, and the SFB VICOM (F41).

¹W. Kohn and L. J. Sham, *Phys. Rev.* **140**, A1133 (1965).

²J. P. Perdew, K. Burke, and M. Ernzerhof, *Phys. Rev. Lett.* **77**, 3865 (1996).

³J. Harl and G. Kresse, *Phys. Rev. Lett.* **103**, 056401 (2009).

⁴A. D. Becke, *J. Chem. Phys.* **98**, 1372 (1993).

⁵J. P. Perdew, M. Ernzerhof, and K. Burke, *J. Chem. Phys.* **105**, 9982 (1996).

⁶C. Adamo and V. Barone, *J. Chem. Phys.* **110**, 6158 (1999).

⁷J. Heyd, G. E. Scuseria, and M. Ernzerhof, *J. Chem. Phys.* **118**, 8207 (2003); **124**, 219906(E) (2006).

⁸A. V. Krūkau, O. A. Vydrov, A. F. Izmaylov, and G. E. Scuseria, *J. Chem. Phys.* **125**, 224106 (2006).

⁹J. Paier, M. Marsman, K. Hummer, G. Kresse, I. C. Gerber, and J. G. Ángyán, *J. Chem. Phys.* **124**, 154709 (2006).

- ¹⁰K. Hummer, J. Harl, and G. Kresse, *Phys. Rev. B* **80**, 115205 (2009).
- ¹¹J. P. Perdew, A. Ruzsinszky, G. I. Csonka, O. A. Vydrov, G. E. Scuseria, L. A. Constantin, X. Zhou, and K. Burke, *Phys. Rev. Lett.* **100**, 136406 (2008).
- ¹²R. Armiento and A. E. Mattsson, *Phys. Rev. B* **72**, 085108 (2005).
- ¹³A. E. Mattsson, R. Armiento, J. Paier, G. Kresse, J. M. Wills, and T. R. Mattsson, *J. Chem. Phys.* **128**, 084714 (2008).
- ¹⁴A. E. Mattsson and R. Armiento, *Phys. Rev. B* **79**, 155101 (2009).
- ¹⁵J. P. Perdew, A. Ruzsinszky, G. I. Csonka, L. A. Constantin, and J. Sun, *Phys. Rev. Lett.* **103**, 026403 (2009).
- ¹⁶J. Harl, L. Schimka, and G. Kresse, *Phys. Rev. B* **81**, 115126 (2010).
- ¹⁷A. Grüneis, M. Marsman, J. Harl, L. Schimka, and G. Kresse, *J. Chem. Phys.* **131**, 154115 (2009).
- ¹⁸A. B. Alchagirov, J. P. Perdew, J. C. Boettger, R. C. Albers, C. Fiolhais, *Phys. Rev. B* **63**, 224115 (2001).
- ¹⁹G. Kern, G. Kresse, and J. Hafner, *Phys. Rev. B* **59**, 8551 (1999).
- ²⁰B. B. Karki, R. M. Wentzcovitch, S. de Gironcoli, and S. Baroni, *Phys. Rev. B* **61**, 8793 (2000).
- ²¹P. E. Blöchl, *Phys. Rev. B* **50**, 17953 (1994).
- ²²G. Kresse and D. Joubert, *Phys. Rev. B* **59**, 1758 (1998).
- ²³G. Kresse and J. Hafner, *Phys. Rev. B* **48**, 13115 (1993).
- ²⁴G. Kresse and J. Furthmüller, *Comput. Mater. Sci.* **6**, 15 (1996).
- ²⁵J. Paier, R. Hirschl, M. Marsman, and G. Kresse, *J. Chem. Phys.* **122**, 234102 (2005).
- ²⁶M. Ernzerhof and J. P. Perdew, *J. Chem. Phys.* **109**, 3313 (1998).
- ²⁷T. M. Henderson, B. G. Janesko, and G. E. Scuseria, *J. Chem. Phys.* **128**, 194105 (2008).
- ²⁸E. Weintraub, T. M. Henderson, and G. E. Scuseria, *J. Chem. Theory Comput.* **5**, 754 (2009).
- ²⁹J. Heyd and G. E. Scuseria, *J. Chem. Phys.* **120**, 7274 (2004).
- ³⁰L. A. Constantin, J. P. Perdew, and J. M. Pitarke, *Phys. Rev. B* **79**, 075126 (2009).
- ³¹M. Marsman, J. Paier, A. Stroppa, G. Kresse, *J. Phys.: Condens. Matter* **20**, 064201 (2008).
- ³²P. Haas, F. Tran, and P. Blaha, *Phys. Rev. B* **79**, 085104 (2009); **79**, 209902(E) (2009).
- ³³G. Kresse, J. Furthmüller, and J. Hafner, *Europhys. Lett.* **32**, 729 (1995).
- ³⁴B. Grabowski, H. Tilmann, J. Neugebauer, *Phys. Rev. B* **76**, 024309 (2007).
- ³⁵See supplementary material at <http://dx.doi.org/10.1063/1.3524336> for detailed data of bulk moduli for 30 solids and atomization energies for the G2-1 test set.
- ³⁶J. Paier, M. Marsman, and G. Kresse, *J. Chem. Phys.* **127**, 024103 (2007).
- ³⁷T. Soma, *J. Phys. C: Solid State Phys.* **11**, 2669 (1978).
- ³⁸W. A. Harrison, *Electronic Structure and the Properties of Solids* (Dover, New York, 1989).
- ³⁹M. Grüning, A. Marini, and A. Rubio, *J. Chem. Phys.* **124**, 154108 (2006).
- ⁴⁰J. P. Perdew, R. G. Parr, M. Levy, and J. L. Balduz, Jr., *Phys. Rev. Lett.* **49**, 1691 (1982).
- ⁴¹A. J. Cohen, P. Mori-Sanchez, and W. Yang, *Phys. Rev. B* **77**, 115123 (2008).
- ⁴²A. Seidl, A. Görling, P. Vogl, and J. A. Majewski, *Phys. Rev. B* **53**, 3764 (1996).
- ⁴³E. Sagvolden, J. P. Perdew, and M. Levy, *Phys. Rev. A* **79**, 026501 (2009).
- ⁴⁴F. Oba, A. Togo, I. Tanaka, J. Paier, and G. Kresse, *Phys. Rev. B* **77**, 245202 (2008).
- ⁴⁵S. Lany and A. Zunger, *Phys. Rev. B* **78**, 235104 (2008).
- ⁴⁶A. Alkauskas, P. Broqvist, and A. Pasquarello, *Phys. Rev. Lett.* **101**, 046405 (2008).
- ⁴⁷H.-P. Komsa, P. Broqvist, and A. Pasquarello, *Phys. Rev. B* **81**, 205118 (2010).
- ⁴⁸J. Heyd, J. E. Peralta, G. E. Scuseria, and R. L. Martin, *J. Chem. Phys.* **123**, 174101 (2005).
- ⁴⁹Y. Zhang and W. Yang, *Phys. Rev. Lett.* **80**, 890 (1998).
- ⁵⁰B. Hammer, L. B. Hansen, and J. K. Norskov, *Phys. Rev. B* **59**, 7413 (1999).
- ⁵¹D. I. Bilc, R. Orlando, R. Shaltaf, G.-M. Rignanese, J. Íñiguez, and Ph. Ghosez, *Phys. Rev. B* **77**, 165107 (2008).